# Photoreceptor complexity accompanies adaptation to challenging marine environments in Anthozoa

Sebastian G. Gornik[‡,1], B. Gideon Bergheim[‡,1], Nicholas S. Foulkes[1,2*] and Annika Guse[1*]

[1] Centre for Organismal Studies, Heidelberg University, Heidelberg 69120, Germany.

[2] Institute of Biological and Chemical Systems, Karlsruhe Institute of Technology, Hermann-von-Helmholtz Platz 1, Eggenstein-Leopoldshafen 76344, Germany.

[‡] These authors contributed equally to this work.

* Corresponding authors (annika.guse@cos.uni-heidelberg.de; nicholas.foulkes@kit.edu)

**Abstract**

Light represents a key environmental factor, which shapes the physiology and evolution of most organisms. Notable illustrations of this are reef-building corals (Anthozoa), which adapted to shallow, oligotrophic, tropical oceans by exploiting light from the sun and the moon to regulate various aspects of physiology including sexual reproduction, phototaxis and photosymbiosis. Together with the Medusozoa, (including jellyfish), the Anthozoa constitute the ancestral metazoan phylum cnidaria. While light perception in Medusozoa has received attention, the mechanisms of light sensing in Anthozoa remain largely unknown. Cnidaria express two principle groups of light-sensing proteins: opsins and photolyases/cryptochromes. By inspecting the genomic loci encoding these photoreceptors in over 35 cnidarian species, we reveal that Anthozoa have substantially expanded and diversified their photoreceptor repertoire. We confirm that, in contrast to Medusozoa, which retained one opsin class, anthozoans possess all three urmetazoan opsin classes. We show that anthozoans also evolved an extra sub-group (actinarian ASO-IIs). Strikingly, we reveal that cryptochromes including CRY-IIs are absent in Medusozoa, while the Anthozoa retained these and evolved an additional, novel cryptochrome class (AnthoCRYs), which contain unique tandem duplications of up to 6 copies of the PHR region. We explored the functionality of these photoreceptor groups by structure-function and gene expression analysis in the anthozoan model species *Exaiptasia pallida* (*Aiptasia*), which recapitulates key photo-behaviors of corals. We identified an array of features that we speculate reflect adaptations to shallow aquatic environments, moonlight-induced spawning synchronization and photosymbiosis. We further propose that photoreceptor complexity and diversity in Anthozoa reflects adaptation to challenging habitats.

## Introduction

Light from both the sun and moon dominates the life of many organisms and has had a profound impact on their evolution. While the mechanisms underlying light sensing have been studied in a comparatively small group of animal models, little is known about the impact of light on the physiology and evolution of more ancestral metazoan groups such as the cnidarians. These are basal, non-bilaterian, eumetazoan animals divided into two major groups, the Anthozoa and the Medusozoa (Figure 1A; [1], which both exploit a complexity of sunlight and moonlight-based cues to regulate various aspects of their physiology and behaviour (Figure 1B). Notable examples of highly light-dependent cnidarians are reef-building corals and anemones (both Anthozoa; Figure 1A), many of which live in an evolutionary ancient symbiotic relationship with eukaryotic, photosynthetic dinoflagellates of the Symbiodiniaceae family [2, 3]. The symbionts use sunlight to provide essential photosynthetically-fixed nutrients to their hosts to support host survival in otherwise oligotrophic tropical oceans. In fact, the nutrient transfer from dinoflagellate symbionts to the reef-building corals powers the productivity of reef ecosystems, which are home to more than 25% of all marine species [4]. The majority of these 'photosynthetic cnidarians' have a sessile lifestyle in shallow sunlit waters and are mobile only during early development at the larval stage (Figure 1B). Due to this almost 'plant-like' lifestyle, sessile cnidarians face similar challenges as true plants such as exposure to intense sunlight, which also bears the risk of temperature stress and UV-induced DNA damage. In addition, most cnidarians harness light from both the sun and moon to orchestrate gamete release during sexual reproduction, including the synchronous mass-spawning events of reef-building corals worldwide [5, 6]. Other important photo-induced behaviours of cnidarians include phototaxis and diurnal migration [7-10]. Given the strong dependence of the cnidarian lifestyle upon environmental lighting conditions, a key question is: which mechanisms mediate these broad ranging effects of light? Given the ecological niches that cnidaria occupy, it is likely that their photoreceptors and light responsive systems would participate in temporally and spatially coordinating behaviour and physiology as well as combating the damaging effects of sunlight. However, with few exceptions including jellyfish eye evolution [11, 12], studies on cryptochrome function in relation to circadian rhythms in *Acropora* and *Nematostella* [13, 14], the light-induced gamete-release in *Clytia hemisphaerica* [15] and a study of opsin evolution in *Hydra* [16], the repertoire and function of cnidarian photoreceptors remains poorly understood.

Two main groups of light sensing proteins exist in metazoans. Opsins are eumetazoan-specific 7-transmembrane G-protein-coupled receptors, which typically incorporate a retinal chromophore and appear to have evolved from ancestral metazoan hormone-responsive receptors [10, 17-19]. In most animal groups they have been shown to function as membrane-

74    bound photoreceptors that mediate visual as well as non-visual light sensing, and trigger
75    intracellular signalling events upon detection of specific wavelengths. The second group,
76    comprising photolyases (PLs) and cryptochromes (CRYs), is a set of highly conserved
77    flavoproteins involved in harvesting light energy to drive the repair of DNA damage as well
78    as regulating the circadian clock in response to light. Specifically, PLs enzymatically repair
79    pyrimidine-pyrimidone (6-4) and cyclobutane pyrimidine dimer (CPD) DNA lesions
80    generated by UV radiation. They were already present in the common ancestors of Bacteria,
81    Archaea, and Eukarya and are classified according to the type of DNA damage that they
82    repair ((6-4) PLs and CPD-PLs) [20-23]. CRYs, which generally lack photolyase enzyme
83    activity, appear to have evolved independently several times from PLs later during evolution
84    in the Eukarya [23-28]. CRY1s are directly light-sensitive and sometimes also referred to as
85    *Drosophila*-type CRYs [29] while CRY2s (also called vertebrate-type CRYs) exhibit no light-
86    dependent function. They instead regulate clock gene transcription in the negative limb of the
87    circadian clock feedback loop [30, 31]. CRY-DASHs ((*Drosophila*, *Arabidopsis*,
88    *Synechocystis*, Human)-type CRYs) are functionally intermediate between PLs and CRYs and
89    considered photoreceptors with residual DNA repair activity [23, 32]. However, all PLs and
90    CRYs share an amino-terminal photolyase-related (PHR) region that contains a DNA-binding
91    photolyase domain (also called alpha/beta domain which binds 5,10-methenyltetrahydrofolate
92    (pterin or MTHF)) and a flavin adenine dinucleotide (FAD) domain, which binds to a FAD
93    chromophore [23].

94

95    In order to explore the function and evolution of these two photoreceptor protein groups in the
96    cnidarian lineage, we have classified extant cnidarian photoreceptors using a detailed
97    phylogenomics approach. Based on this phylogenetic analysis, we investigate the expression
98    and regulation of cnidarian photoreceptors in the anthozoan symbiosis model *Exaiptasia*
99    *pallida* (commonly *Aiptasia*) [33]. *Aiptasia* is widely used to investigate the molecular
100   mechanisms underlying cnidarian-dinoflagellate symbiosis establishment and maintenance
101   [34-38] as well as its breakdown, a phenomenon known as 'coral bleaching' [39]. Moreover,
102   analogous to most corals, *Aiptasia* also exhibits synchronous, blue (moon) light induced
103   gamete release [40] to produce motile larvae that have to find a suitable niche for their light-
104   dependent lifestyle (Figure 1B). Here we reveal a large and highly diverse photoreceptor
105   repertoire in Anthozoa, and in particular in *Aiptasia*, paving the way to dissecting
106   photoreceptor evolution and function to reveal fundamental principles of how cnidarians
107   adapt to their light-dominated environments.

108

109

110   **Results**

### *Opsin complexity in Cnidaria*

111

112 As a first step towards a better understanding of the evolution of the opsin gene family in

113 cnidarians, we generated a detailed molecular phylogeny, based on RNA sequence data and

114 gene structure analysis. Originally, only two types of opsins, the ciliary (c-opsins) and the

115 rhabdomeric (r-opsins) were described [41]. The c-opsins serve as the main visual

116 photoreceptors in vertebrates, while the r-opsins play the same role in invertebrates. Since

117 then, taking advantage of an enormous increase in available sequencing data, new molecular

118 phylogenies and functional studies, more opsin classes have been defined. To date, ten

119 distinct opsin classes have been identified across all Metazoa, three of which, namely the

120 cnidopsins as well as the Anthozoan-specific opsins I (ASO-I) and II (ASO-II) occur in

121 cnidarians (Figure 2A; [42]). The cnidopsins are relatively well studied and are often

122 expressed in a distinct tissue- and stage-specific manner. For example, cnidopsin expression

123 has been studied in the light-sensitive cilia of jellyfish (Medusozoa) eyes, in the hydrozoan

124 battery complex and more ubiquitously in sensory nerve cells [9, 11, 12, 43]. However, far

125 less is known about the anthozoan-specific ASO-I and ASO-IIs; both of which are restricted

126 to Anthozoa (including sea anemones and corals that lack comparable eye-like sensory

127 organs) but are absent in the Medusozoa. Moreover, due to a lack of extensive taxon

128 sampling, a sophisticated assessment of function and diversity for the ASO-I and ASO-II

129 opsins has been lacking. To address this issue, we mined genomic data from 36 cnidarians (7

130 Anthozoa and 29 Medusozoa). Our new, large-scale phylogeny resolves the ten previously

131 identified distinct opsin classes including the three cnidarian types (Figure 2A). All cnidarians

132 (Anthozoa and Medusozoa) possess cnidopsins, which are monophyletic and sister to the

133 animal xenopsins. The monophyletic ASO-I group appears ancestral to all other opsins and

134 has likely been lost secondarily, similar to the loss of ASO-II opsins in the Medusozoa

135 (Figure 2A;[42]). Moreover, our extended analysis revealed that the ASO-II opsins comprise

136 two distinct, previously not formally described sub-clusters (see Vöcking et al. (2017)). We

137 noticed that one of these two clusters exclusively contains opsins from sea anemones

138 *(Actiniaria)*, while the second cluster contains genes from all Anthozoa including sea

139 anemones and corals. This distinct split was confirmed using a second round of reciprocal

140 BLAST searches and phylogenetic inference against a more extensive number of ASO-IIs

141 using data from Picciani et al. (2018) (Figure 2B). Accordingly, we have named the

142 *Actiniaria* (sea anemone)-specific cluster 'actiniarian ASO-IIs' while the second cluster

143 remains ASO-IIs. Intron phase analysis corroborates the ASO-II and Actiniarian ASO-II split

144 since we revealed that genes in both clusters have a single intron at distinct positions

145 (Supplementary Figure 1A). Moreover, we observe that the ASO-I and ASO-II intron

146 distribution is distinct from the ctenopsin and c-opsin intron distribution despite their

147 common ancestry since there is a lack of any conserved homologous intron positions

4

148     (Supplementary Figure 1A). This suggests that the ancestral intron-less ASO-II gene
149     duplicated and subsequently each gene acquired a distinct intron before the ASO-II sub-
150     clusters further diversified.

151

152     Changes in amino acid sequence involving key residues is a hallmark of opsin evolution and
153     functional diversification [17, 44-47]. To assess the overall sequence diversity of the opsins
154     occurring in cnidaria, we used pairwise identity mapping of more than 500 opsins (including
155     237 cnidarian opsins). We found that at the protein level most cnidarian opsins are indeed
156     highly diverse (Supplementary Figure 2). For example, while the ancestral ASO-Is cluster
157     tightly and form one distinct group with a highly similar amino acid composition, the
158     cnidopsins and ASO-IIs are subdivided into various clusters which are interspersed with
159     several classes of opsins associated with higher animals including, for example, vertebrate-
160     specific c-opsins (Supplementary Figure 2). Opsin amino acid composition and photosensory
161     function are highly correlated and specific amino acid residues interact with the chromophore
162     to tune peak spectral sensitivities [44, 48]. Therefore, the high levels of diversity we observe
163     in cnidarian opsins may reflect photosensory diversity rather than being the result of
164     synonymous gene duplications that merely created functionally identical opsin paralogs.

165

166     Interestingly, we specifically noted that opsins within the two ASO-II clusters differ in one
167     major functional amino acid. Typically, opsins contain a highly conserved glutamate residue
168     at position 181 (E181), which stabilizes retinal, the light-sensitive chromophore forming a so-
169     called protonated Schiff base (PSB) when bound to opsin. Light absorption triggers retinal
170     *cis*-to-*trans* isomerization, which, in turn, results in opsin conformational changes that reveal
171     a cytoplasmic G-protein binding site and thereby enables the activation of signalling cascades.
172     Free retinal is maximally sensitive to UV light but its absorption maximum is shifted towards
173     visible light when covalently bound to opsins, ensuring its maximal sensitivity lies within the
174     visual spectrum [17]. However, while most actiniarian ASO-IIs, similar to the cnidopsins and
175     ASO-Is, indeed have a glutamate [Q] at the equivalent position, all members of the
176     anthozoan-wide occurring ASO-IIs sub cluster lack this conserved feature (Figure 2C;
177     Supplementary Figure 1B). To date, E181 has been found to be conserved in all opsins [48,
178     49] with the exception of vertebrate visual opsins where it occurs together with, or is replaced
179     by E113 [17, 47, 50-53], a vertebrate-specific feature associated with even higher fidelity
180     visual photoreception. Interestingly, one *Aiptasia* ASO-II (ASO-II.4) contains both E113 and
181     E181 (Supplementary Figure 1B), suggesting that this presumed vertebrate-specific feature
182     may also have arisen independently in some cnidarians and so may represent an example of
183     convergent evolution conferring higher-fidelity photoreception [53]. Furthermore, these

184 specific amino acid differences are consistent with functional diversification during evolution

185 of the ASO-II opsin group.

186

187 ***Life-stage, symbiotic state and tissue type-specific opsin expression in Aiptasia***

188 In the model species *Aiptasia,* we identified 18 distinct opsins: 4 cnidopsins

189 (XP_020899757.1, XP_020913977.1, XP_020904301.1, XP_020897723.2), 2 ASO-Is

190 (XP_020902074.1, XP_028515325.1) and 5 ASO-IIs (XP_020903100.1, AXN75743.1,

191 XP_020897790.2, XP_028514120.1, XP_020909716.1) and 7 actiniarian ASO-IIs

192 (XP_020914799.1, XP_020906239.1, XP_020909580.1, XP_020907384.1, XP_020910007.1,

193 XP_020893775.2, XP_020914907.2). See also: Supplementary File 1. To assess whether this

194 broad opsin repertoire is actively expressed and if so, during which life stages, we compared

195 opsin expression levels using publicly available *Aiptasia* RNA-Seq data [34, 54]. We found

196 that with one exception, all *Aiptasia* opsins are ubiquitously expressed in both larvae and

197 adults with expression levels of some opsins elevated specifically in adults and others during

198 larval stages suggesting the existence of opsins with larval- and adult-specific functions

199 (Figure 3A). Likewise, opsin expression varies depending on the symbiotic state (Figure 3B).

200 For example, one opsin from the actiniarian-specific ASO-II group (ASO-II.12, dark green),

201 and two from the ASO-II group (ASO-II.7 and ASO-II.11, yellow) show significantly higher

202 expression levels in symbiotic anemones when compared to their aposymbiotic (non-

203 symbiotic) counterparts. This is consistent with previous findings that symbiotic association

204 influences photo-movement in *Aiptasia* [8] and suggests that host perception of

205 environmental light by opsin-mediated light-sensing may change in response to symbiosis, for

206 example to adjust the levels of sunlight exposure for optimal photosynthesis rates.

207

208 Opsins have been implicated in 'sensing' moonlight to synchronize gamete release in corals

209 [5, 55]. Specifically, it is predicted that physiologically relevant blue shifts in the irradiance

210 spectrum measurable during twilight on several days before and after the full moon acts as a

211 trigger for a potential opsin-mediated dichromatic visual system where readouts from a blue-

212 and red-light sensitive opsin are integrated to induce spawning [6]. Accordingly, exposure for

213 5 nights to LED-based blue light has been shown to specifically induce synchronized

214 spawning in *Aiptasia* [40]. By analogy with the jellyfish *Clytia hemisphaerica* in which the

215 opsin relevant for spawning is specifically expressed in the gonadal tissue [15], we therefore

216 asked whether any of the opsin genes present in *Aiptasia* showed a gonad-specific expression

217 pattern (Supplementary Figure 3). By using qPCR analysis, we revealed that *Aiptasia* ASO-

218 II.3 is indeed expressed in a tissue-specific manner and significantly up-regulated in

219 mesenteries when compared to the tentacles (Figure 3C). Thus, *Aiptasia* ASO-II.3 represents

220 a candidate opsin that may be involved in spawning induction in this species.

221

### *Novelty in the cnidarian photolyase and cryptochrome repertoire*

222 *Novelty in the cnidarian photolyase and cryptochrome repertoire*

223 Another major group of light-sensing proteins in animals are the CRY and PL flavoproteins,

224 however, to date their phylogeny in cnidarians has not been assessed in detail. To address this

225 issue, we next used phylogenomic analysis and considered the position of conserved introns.

226 We revealed that while they possess CRY-DASH, CPD-II PLs and (6-4) PLs, CPD-Is and

227 CRY-Is are absent from all cnidarians (Figure 4A, Supplementary Figure 4A). Furthermore,

228 while CRY-IIs are encountered only in the subphylum Anthozoa, strikingly CRYs are

229 completely absent from the Medusozoa that are represented by 29 taxa in our analysis

230 (Supplementary File 5).

231

232 Interestingly, we have identified two distinct CRY groups in Anthozoa. One is a sister group

233 to 'animal CRY-IIs' that we named anthozoan CRY-IIs. Due to their phylogenetic position at

234 the base of animal CRY-IIs we speculate these are likely to be involved in circadian clock

235 function [29, 56, 57]. However, a second, novel CRY group appears to be basal to both (6-4)

236 PLs and 'animal CRY-IIs' (but distinct from CRY-Is and sponge CRYs). We thus named this

237 group Anthozoan-specific CRYs (AnthoCRYs) (Figure 4A and 4B). Previous, preliminary

238 analysis of both cryptochrome groups lead to them being classified within the animal CRY-

239 IIs, presumably due to a lack of cnidarian taxa representation in associated phylogenies [13,

240 58, 59]. Our study now clarifies their phylogenetic position and proposes their name based on

241 identity. Thus, similar to the situation for the opsin genes, the Anthozoa possess a more

242 extensive repertoire of CRYs when compared with the Medusozoa.

243

244 A hallmark of PLs and CRYs is the PL-homologous region (PHR region) that contains a N-

245 terminal DNA-binding photolyase domain (also called the alpha/beta domain) and a C-

246 terminal FAD chromophore binding domain [21, 22, 57]. All PLs and CRYs described to date

247 contain a single PHR region. Strikingly, however, here we reveal that AnthoCRYs contain up

248 to six tandemly repeated PHR regions (Figure 4B). We confirmed this PHR region

249 duplication independently in the sea anemone *Aiptasia* by PCR and sequencing (Figure 4C) of

250 the *Aiptasia* AnthoCRY.1 cDNA. Such a PHR region expansion has not been described for

251 any PL or CRY to date. This expansion occurs across all Anthozoa including non-symbiotic

252 and symbiotic members indicating that the tandem duplication of PHR domains in Anthozoan

253 CRYs might serve a common purpose in this animal group. Interestingly, it appears to be

254 absent from *Nematostella*.

255

### *Light regulated CRY gene expression in Cnidaria*

256 *Light regulated CRY gene expression in Cnidaria*

7

257   We next wished to investigate the functionality of these flavoprotein genes in terms of their
258   regulation following light exposure. In many animal groups the expression of CRY and PL
259   genes is induced upon exposure to light as a key mechanism to regulate the circadian clock or
260   to upregulate DNA repair capacity in response to prolonged sunlight exposure. Consistently,
261   in *Nematostella* three CRYs have been reported, two of which are upregulated in response to
262   light [59]. Similarly, at least two different CRYs (Cry1a (XP_001631029) and Cry1b
263   (XP_001632849)) are expressed in a light dependant manner in the coral *A. millepora* [13]. In
264   the sea anemone *Aiptasia diaphana* two CRYs were identified (without accession numbers)
265   and shown to be expressed rhythmically in the presence of a day-night cycle [60]. We
266   therefore explored to which extent light regulates the 8 different *Aiptasia* PL and CRY genes
267   that we identified (2 CPD_II isoforms (XP_020910442.1, XP_020910516.1), 1 CRY-DASH
268   (XP_020903321.1), 2 (6-4) PL isoforms (XP_020915076.1, XP_020915067.1), 1 Anthozoan
269   CRY (XP_020904995.1) and 2 AnthoCRYs (XP_020902079.1, XP_020917737.1; see also:
270   Supplementary File 2). With the exception of AnthoCRY.2, where mRNA levels are
271   undetectable in *Aiptasia* larvae, we showed that all CRY and PL genes are generally
272   ubiquitously expressed in both *Aiptasia* larvae and adults (Supplementary Figure 4B). We
273   next adapted *Aiptasia* for 4 days to constant darkness and then exposed them for a period of 8
274   hours to light, sampling at 2-hours intervals. Our results revealed that the expression of
275   *Aiptasia* PLs and CRYs was differentially affected by light exposure. Specifically, *Aiptasia*
276   CPD-II, *Aiptasia* DASH-CRY and *Aiptasia* (6-4) PL were largely unresponsive to light
277   treatment (Figure 5A to 5C). In contrast, AnthoCRYs and CRY-II expression was rapidly
278   induced upon exposure to light (Figure 5D to 5F).

279

280   A light-inducible expression pattern may be the consequence of acutely light-driven gene
281   expression or alternatively of regulation by the circadian clock that is also likely to be
282   synchronized during the period of light exposure. To distinguish between these two
283   possibilities, we tested AnthoCRY and CRY-II expression by exposing *Aiptasia* to light-dark
284   (LD) cycles and then transferring animals to constant darkness (DD). Clock regulation would
285   be revealed by the appearance of rhythmic expression under an LD cycle that would persist
286   following transfer to constant darkness. Therefore, samples were prepared at 6 hours intervals
287   during either exposure to an LD cycle or immediately following transfer from LD to DD
288   conditions and then CRY gene expression was assayed by qPCR. Under LD conditions we
289   observed rhythmic expression with elevated expression during the light period, peaking at 8
290   hours after lights on, and then decreasing during the dark period, with a trough at 8 hours after
291   lights off (Figure 5G to 5I). In contrast, immediately upon transfer to DD conditions,
292   rhythmic expression was absent, showing that changes in CRY gene expression are indeed
293   light-, rather than clock-driven (Figure 5G to 5I).

8

294

295     We have previously studied the mechanisms underlying light-driven gene expression of

296     cryptochromes and photolyases in vertebrates [61, 62]. We revealed a conserved role for

297     light-induced transcription of these genes, mediated by the D-box element, an enhancer that

298     has also been associated with circadian clock regulation together with the E-box enhancer

299     [63]. We therefore tested whether D-box or E-box enhancer elements might be encountered

300     within the promoter regions of the various *Aiptasia* CRY and PL genes. By scanning the

301     genomic regions 1 kb upstream of the respective gene START codon (ATG), single D-box

302     enhancers were identified in 6-4 PL and CPD-II, two genes which were not induced upon

303     exposure to light. However, in the case of the light-inducible AnthoCRY and CRY-II genes

304     we identified several PAR/bZIP binding sites (D-boxes; Figure 5J), interestingly, located

305     proximally to E-box enhancers. Furthermore, consistent with the existence of functional D-

306     box regulatory pathways in Anthozoa, we show that *Aiptasia* possesses 4 putative orthologs

307     of the PAR/bZIP TFs family (three TFs basal to Hepatic leukemia factor (HLF)-type

308     PAR/bZIP TFs and one DBP (D-box Binding PAR/bZIP) TF (Supplementary Figure 5) which

309     have been shown to bind to and regulate transcription from the D-box enhancer in vertebrates

310     [64-66].

311

312     **Discussion**

313     Reef-building corals and sea anemones represent critically important members of the

314     ecosystems in shallow, oligotrophic, tropical oceans. Their physiology is dominated by light.

315     They exploit sunlight and moonlight to regulate their sexual reproduction, phototaxis and

316     photosymbiosis. Furthermore, there exposure to sustained high levels of sunlight puts them at

317     particular risk from elevated levels of DNA damage. In order to explore the molecular

318     mechanisms linking light with anthozoan biology, we present the first detailed phylogenetic

319     analysis of two major light sensing protein groups: the opsins and the

320     cryptochrome/photolyase flavoproteins. Within the broader context of the ancestral metazoan

321     phylum, the cnidaria, we reveal that the Anthozoa have substantially expanded and diversified

322     their photoreceptor repertoire compared with the Medusozoa. This striking observation raises

323     several fundamental questions concerning how this expanded photoreceptor capacity may be

324     linked with adaptation to their extreme, shallow water environments.

325     *The origins of opsin diversification in the Cnidaria*

326     The last common ancestor of the cnidaria and bilateria possessed three classes of distinct

327     opsins giving rise to the cnidopsins, ASO-Is and ASO-IIs, yet the Medusozoa only retained

328     the cnidopsins. The extant Anthozoa on the other hand possess multiple ASO-Is and

329  substantially expanded and diversified the ASO-IIs. The ASO-I is the most ancient opsin

330  class in the metazoan lineage and represents phylogenetically and, based on protein sequence,

331  a coherent group, but to date its function is entirely unknown. Interestingly, the ASO-IIs are

332  much more diverse at the sequence level and share a common ancestry with the tetraopsins

333  and r-opsins as well as to the cnidopsins, xenopsins, ctenopsins and the well-studied c-opsins

334  responsible for visual photoreception in vertebrates. This suggests that an urmetazoan animal

335  possessed an ancestral but now extinct opsin that early in opsin evolution gave rise to multiple

336  opsin classes.  Frequent lineage-specific gains and losses then shaped the broad repertoire of

337  light-sensing mechanisms and opsin classes that we see to date [12, 42, 67]. This capacity for

338  diversity is still reflected by the novel ASO-II sub-cluster that is restricted to anthozoan

339  anemones. Interestingly, if cnidopsins are indeed early xenopsins as suggested by our study

340  and also Ramirez et al. (2016) and if ASO-IIs are indeed sister to the c-opsins as suggested

341  here and by Ramirez et al. (2016) and Vöcking et al. (2017) the cnidarians may be the only

342  animals where xenopsins and c-opsins (or at least their direct ancestral cousins) co-occur.

343  In accordance with the notion that ASO-IIs play an important role in the adaptation of

344  Anthozoa, to their environments, we find that the highly conserved E181 amino acid residue

345  is absent in the ASO-IIs suggesting that this key position has been modified, possibly to shift

346  the ASO-IIs wavelength specificity more towards blue light (shorter wavelengths) absorption

347  which may be a specific adaptation to aquatic marine environments where the penetration of

348  longer wavelengths is reduced with increasing water depth [68, 69]. Indeed, by using

349  computational modelling based on a vertebrate opsin crystal structure, it was shown that loss

350  of E181 causes a light absorption shift of more than 100 nm towards blue light [70]. In the

351  future, a functional analysis of the wavelength specificities of anthozoan opsins will provide

352  fundamental new insight into the ability of basal animals to exploit various light cues.

353

354  ***Adaptations to light-induced sexual reproduction***

355  Coral sexual reproduction is a vital process for species viability. It is key for genetic diversity,

356  dispersal by motile larvae and affects the abundance of juvenile corals to replenish aging

357  coral communities. However, for sessile Anthozoa such as reef-building corals, achieving

358  efficient fertilization rates is challenging because it occurs effectively only a few hours after

359  gamete release by the parental colonies and gametes are easily diluted within the open space

360  of the ocean. Accordingly, corals have evolved a precise spawning synchrony within

361  populations integrating various environmental cues including temperature and solar irradiance

362  to set the exact month, lunar cycles to set the exact night and circadian light cues to set the

363  exact hour (see [71] and references therein). In this context it is worth noting that *Aiptasia*

364  recapitulates key aspects of light-induced synchronized spawning observed in corals. Under

365    laboratory conditions, delivery of LED-based blue-light for 5 consecutive nights, simulating
366    full moon, triggers gamete release peaking 9-10 days after the last exposure to blue light. This
367    effect is wavelength-specific as it works effectively with light at 400-460nm, while white
368    light is ineffective [40]. Gamete release occurs ~5.5h after 'sunset' and after release,
369    fertilization efficiency drops from 100% to ~25% within the first hour [72] underlining the
370    need for precise timing of sexual reproduction within the Anthozoa.

371

372    Opsins have been implicated as light-sensors to trigger spawning in corals [5, 6, 73].
373    Moreover, a functional relationship between a light-induced, opsin-dependent spawning
374    mechanism has been shown in a medusozoan, the jellyfish *Clytia hemispherica*. This elegant
375    study found that a gonadal opsin senses blue light to trigger spawning upon dark-light
376    transitions [15]. Thus, it is tempting to speculate that *Aiptasia* ASO-II.3, which is also
377    expressed at elevated levels in gonads (Figure 3C) may serve a similar function for
378    synchronous gamete release in this anthozoan species. *Aiptasia* represents a tractable model to
379    experimentally dissect the mechanisms of light-induced sexual reproduction in Anthozoa
380    including the integration of lunar cycles as well circadian periodicities to trigger gamete
381    maturation and synchronous release. A mechanistic understanding of how Anthozoa have
382    adapted the timing of sexual reproduction to their environments, together with analysing how
383    environmental changes affect the spawning synchronicity within the ecosystem, is key to
384    direct future research and conservation efforts [71].

385

386    ***Adaptations to increased UV-induced DNA damage***
387    Our results have also revealed significantly more diversity of the CRY/PL flavoproteins in the
388    Anthozoa compared with the Medusozoa. While both contain CRY-DASH, CPD-II PLs and
389    (6-4) PLs, Anthozoa also have two extra CRY classes (AnthoCRYs and Anthozoan CRYIIs),
390    which are absent from Medusozoa. Thus, strikingly, the Medusozoa completely lack CRY
391    genes. The AnthoCRYs represent a phylogenetically well-supported but previously
392    unidentified, anthozoan-specific CRY family, which resolves at the base of animal CRY-IIs
393    and (6-4) PLs. A hallmark of all CRY/PL proteins analysed to date is the highly conserved
394    structure of the PHR domain consisting of a N-terminal domain and a FAD domain.
395    However, here we reveal that the anthozoan AnthoCRYs exhibit an extensive and
396    unprecedented PHR region duplication. Tandemly repeated PHR regions have never been
397    observed before in any other eukaryotic or prokaryotic species. While the structure and
398    function of the PHR has been studied in great deal in the context of PLs revealing its light-
399    dependant DNA-repair function, the role of the PHR region in the CRYs remains rather
400    unclear [21]. Nevertheless, until this current report, only single PHR regions have been

401    scrutinized in PL or CRY proteins. The identification of tandem duplication of the PHR

402    region in Anthozoa provides some tantalizing clues as to the functional significance of this

403    domain. It is tempting to speculate that AnthoCRYs, which are clearly distinct from

404    vertebrate CRY-IIs and CRY-Is and sister also to (6-4) PLs, have not yet lost their light-

405    dependant DNA repair activity and in fact have evolved in the Anthozoa to provide higher

406    UV-damage repair capacities reflected by their domain duplications. Furthermore, the

407    observation that both AnthoCRY.1 and AnthoCRY.2 exhibit light-inducible expression would

408    also be consistent with these genes playing a key role in the response to intensive sunlight

409    exposure, a threat that sessile corals likely face on a daily basis in their sunlit tropical habitats.

410    *Adaptations of the circadian clock during cnidarian evolution*

411    Transcriptional control of gene expression in response to light serves as a central regulatory

412    element within the circadian clock core mechanism. This enables regular adjustment of the

413    phase of the circadian clock to match that of the environmental day-night cycle. In non-

414    mammalian vertebrates D-boxes mediate light-inducible gene expression, alone or in

415    combination with other enhancers such as the E-box [61-63]. Furthermore, in fish, D-boxes

416    also activate transcription in response to oxidative stress and UV exposure [64]. Thus, in the

417    majority of vertebrates, D-boxes coordinate the transcription of a set of genes that includes

418    certain clock genes as well as genes involved in the repair of UV-damaged DNA [61, 64] to

419    constitute a cellular response to sunlight exposure. This contrasts with the situation of

420    mammals where D-boxes exclusively direct clock-controlled rhythms of gene expression

421    [74]. Therefore, the discovery of an enrichment of proximally spaced E and D-box enhancer

422    elements in the promoters of the light inducible AnthoCRY genes supports the view that the

423    D-box plays an ancestral sunlight-responsive role. Furthermore, this may also predict a

424    function for AnthoCRYs in the complex cellular response to the damaging effects of sunlight

425    which may involve responses to visible and UV light as well as oxidative stress.

426

427    CRYs are key regulators of the circadian clock in animals. Together with the Period proteins

428    they serve as negative regulators within the core transcription-translation feedback loop

429    mechanism [30]. Based on previous studies of plant and animal circadian clocks, it can be

430    predicted that clock function is of fundamental importance for many anthozoan species. For

431    example, the adaptation of the host cell physiology to the daily cycles of photosynthetic

432    activity of the dinoflagellate symbionts as well as the sessile lifestyle of Anthozoa is likely to

433    rely heavily on this endogenous timing mechanism that anticipates the course of the day-night

434    cycle. This may well account for the conservation of CRY function in the Anthozoa. The

435    absence of CRY in Medusozoa suggests that in these species, circadian clocks may be based

436    upon fundamentally different mechanisms. Interestingly, canonical circadian clock genes

437    were previously reported to be absent in *Hydra* and possibly all Medusozoa [7, 73, 75, 76].

438    However, whether medusozoan species have evolved alternative mechanisms to control

439    rhythmic behaviour and physiology, or whether they may have actually lost circadian clock

440    function represents a fascinating topic for future investigation.

441

442    ***The origins of photoreceptor diversification***

443    One key difference between the Anthozoa and Medusozoa is that Medusozoa have a free-

444    swimming medusa phase during their lifecycle, while Anthozoa do not. Instead, Anthozoa are

445    typically sessile animals, which are only motile during larval stages (Figure 1A). Possibly

446    connected with this fundamental difference is that the Anthozoa lack eyes. Thus, we speculate

447    that the evolution of relatively sophisticated eye-like structures based on light-sensitive cilia

448    expressing cnidopsins allows for the integration of various light cues simultaneously in

449    Medusozoa. Instead, in the Anthozoa the repertoire of non-visual opsins expanded in order to

450    perceive light in different photic environments and during distinct life stages. This expansion

451    could allow fine-tuning of animal physiology and behaviour including gamete release and

452    phototaxis as well as optimizing conditions for their photosynthetic symbionts. Another

453    striking example of how the expansion and sequence diversification of opsins allows

454    adaptation to specific environments has recently been elucidated in deep-sea fish. While

455    classically all vertebrates rely on only a single rod opsin rhodopsin 1 (RH1) for obtaining

456    visual information in dim light conditions, some deep-sea fish have independently expanded

457    their single RH1 gene to generate multiple RH1-like opsins that are tuned to different

458    wavelengths of light by modulating key functional residues [44].

459

460    Our demonstration that eighteen distinct opsins and eight distinct PLs and CRYs are

461    expressed in *Aiptasia*, in either larval or adult stages, in symbiotic or aposymbiotic animals, in

462    a tissue-specific manner and in some cases, in a light inducible manner suggests that

463    symbiotic anthozoans possess a remarkable, functional diversity in their photoreception

464    mechanisms. The augmented complexity of photoreceptors in the Anthozoa is likely due to

465    gene loss in the Medusozoa as well as to continued gene expansion and diversification within

466    the Anthozoa and is indicative of distinct light-sensing mechanisms associated with different

467    lifestyles. It may well be that the increased photoreceptor diversity of Anthozoa including

468    corals and sea anemones represents an essential adaptation to their predominantly sessile

469    lifestyle. Ultimately, complex light sensing mechanisms may permit the integration of sun

470    and moon light to regulate physiology and behaviour, and to facilitate adaptation to their

471    challenging environments: shallow, highly sunlit, tropical oceans where food is scarce and

472    there is an enhanced risk of UV-induced DNA damage (Figure 1B). However, to date, no

473    anthozoan-specific photoreceptor has been functionally characterized. Here we have

474  generated an essential framework to experimentally analyse this diverse repertoire of non-
475  visual photoreceptors using *Aiptasia* as a tractable model. A functional characterization of
476  photoreceptors to uncover the mechanisms of light-sensing of cnidarians will provide
477  profound new insight into the basic principles whereby metazoans adapt to light-dominated
478  environments and how distinct lifestyles shape their photoreceptor repertoires.

479

480  **Materials and Methods**

481  ***Aiptasia* culture and spawning**

482  *Aiptasia* stocks were cultured as described [40]. Briefly, animals were reared from pedal
483  lacerates for at least 6 months. For the spawning experiments, animals with a pedal disc
484  diameter of 1 cm were separated into individual, small-sized, food-grade translucent
485  polycarbonate tanks (GN 1/4– 100 cm height, #44 CW; Cambro, Huntington Beach, USA)
486  filled with artificial seawater (ASW) (Coral Pro Salt; Red Sea Aquatics Ltd, Houston, USA or
487  REEF PRO; Tropic Marin, Switzerland) at 31-34 ppt salinity at 26°C. They were fed with
488  *Artemia salina* nauplius larvae 5 times a week during the entire experimental period. ASW
489  was exchanged twice per week and the tanks were cleaned using cotton tipped swabs as
490  required.

491

492  ***Sampling regimes***

493  *Circadian rhythmicity of CRY/PL expression*

494  Firstly, *Aiptasia* polyps were adapted for 4 days to constant darkness and then exposed to
495  light from white fluorescent bulbs with an intensity of ~20-25 μmol m$^{-2}$ s$^{-1}$ of
496  photosynthetically active radiation (PAR), as measured with an Apogee PAR quantum meter
497  (MQ-200; Apogee, Logan, USA) for a period of 8 hours, sampling at 2-hour intervals.
498  Additionally, *Aiptasia* polyps were exposed to light-dark (LD, 12 h:12 h) cycles and then
499  transferred to constant darkness (DD), sampling at 2, 8, 14 and 20 hours (LD) and 26, 32, 38
500  and 44 hours (DD).

501

502  **Computational methods**

503  *Identification of CRY, PL and opsin photoreceptors and PAR/bZIP transcription factor*
504  *homologs*

505  Potential CRY, PL and opsin sequences were recovered from *Aiptasia* genomic data (NCBI
506  Bioproject PRJNA261862; [54]) by searching for annotation keywords and BLAST search
507  using specific query sets. For opsins we used bovine (P51490), *Acropora palmata* (L0ATA4),
508  *Carybdea rastonii* (B6F0Y5), honeybee (B7X752) and *Clytia hemisphaerica* (A0A2I6SFS3)
509  opsins. For PLs and CRYs queries we used a set off previously published well-defined
510  CRY/PL proteins, which we expanded to include known sponge and anthozoan CRYs [58,

14

511    77]. A set of known vertebrate PAR/bZIP transcription factors (TFs) were used as query sets

512    to identify *Aiptasia* PAR/bZIP homologues using BLAST searches. The longest ORFs from

513    recovered putative opsin genes were translated and aligned with the query sequences using

514    ClustalW (GONNET, goc = 3, gec = 1.8). For opsins, sequences, which did not contain lysine

515    K296, which is essential and indicative of chromophore binding, were excluded. For *Aiptasia*

516    genes, we noticed that some of the associated gene models contained Ns (resulting in Xs in

517    their amino acid sequences). Thus, we verify existing gene models by mapping reads from

518    published short read RNA-seq libraries (Adult-apo: SRR1648359, SRR1648361,

519    SRR1648362; Adult-intermediate: SRR1648363, SRR1648365, SRR1648367, SRR1648368;

520    Adult-sym: SRR1648369, SRR1648370, SRR1648371, SRR1648372; Larvae-apo:

521    SRR1648373, SRR1648374; Larvae-sym: SRR1648375, SRR1648376) to these gene models

522    using HiSAT2 (https://ccb.jhu.edu/software/hisat2/index.shtml) at standard settings [78].

523    Uniquely mapped reads were extracted using samtools 1.2 and sequences then manually

524    curated prior to alignment and phylogenies (Supplementary Files 1-3).

525

526    *Phylogenetic analyses*

527    A custom in-house BLAST database comprising more than 70 eukaryotic genera including

528    *Nematostalla vectensis*, *Pocillopora*, *Stylophora*, *Orbicella*, *Acropora millepora*, *A. digitifera*,

529    *Exaiptasia pallida (Cnidaria, Anthozoa)*, *Abylopsis tetragona*, *Aegina citrea*, *Agalma*

530    *elegans*, *Alatina alata*, *Atolla vanhoeffeni*, *Aurelia aurita*, *Calvadosia cruxmelitensis*,

531    *Cassiopea xamachana*, *Chironex fleckeri*, *Chrysaora fuscescens*, *Clytia hemisphaerica*,

532    *Craseoa lathetica*, *Craspedacusta sowerbyi*, *Craterolophus convolvulus*, *Cyanea capillata*,

533    *Ectopleura larynx*, *Haliclystus sanjuanensis*, *Hydractinia echinata*, *H. polyclina*, *Hydra*

534    *oligactis*, *H. viridissima*, *H. vulgaris*, *Leucernaria quadricornis*, *Nanomia bijuga*, *Physalia*

535    *physalis*, *Podocoryna carnea*, *Stomolophus meleagris*, *Tripedalia cystophora*, *Turritopsis sp*

536    *SK-2016 (Cnidaria, Medusozoa)*, *Aplysia californica (Mollusca)*, *Amphimedon queenslandica*

537    *(Porifera)*, *Caenorhabditis elegans (Nematoda)*, *Drosophila melanogaster (Athropoda)*,

538    *Homo sapiens*, *Mus musculus*, *Danio rerio*, *Xenopus laevis* (all *Vertebrata*), *Monosiga*

539    *brevicollis (Choanoflagellate)*, *Pleurobrachia bachei (Ctenophora)*, *Saccoglossus*

540    *kowalevskii (Hemichordata)*, *Strongylocentrotus purpuratus (Echinodermata)*,

541    *Saccharomyces cerevisiae (Fungi)*, *Toxoplasma gondii*, *Plasmodium falciparum*, *Perkinsus*

542    *marinus*, *Tetrahymena thermophila* (all *Alveolata*) and *Trichoplax adherens (Placozoa)* were

543    used to generate a CRY/PL dataset for phylogenetic analysis. The majority of cnidarian

544    sequences were obtained from published transcriptomes [79], but manually curated and

545    translated in KNIME using in-house workflows comprising EMBOSS *getorf*. All other

546    sequences were obtained from NCBI. For opsin phylogenies existing datasets were modified

547    replacing *Exaiptasia* sequences with our newly verified *Aiptasia* opsin set [15, 42]. Outgroups

548 were defined according to Vöcking et al. (2017) comprising several GPCR receptor family
549 members (melatonin, octopamine, serotonin and adrenergic receptors) and Trichoplax opsin-
550 like sequences, which all belong to class α rhodopsin-like GPCRs. For the detailed analysis of
551 the ASO-II subtypes, additional ASO-II candidates were identified from the same database
552 used for CRY/PL phylogenies using the previously identified *Aiptasia* ASO-IIs as query.
553 Longest ORFs from recovered putative *Aiptasia* PAR/bZIP genes were translated and aligned
554 to query sequences comprising multiple metazoan PAR/bZIPs and a CEBP (CCAAT-
555 enhancer-binding proteins) outgroup. In all cases sequences were aligned using ClustalW
556 (GONNET, goc: 3, gec: 1.8). Automated trimming was performed using trimAI using
557 standard parameters [80]. Unstable leaves were identified and excluded using phyutilities
558 with "-tt 100" settings [81]. Best-fitting amino acid substitution models were determined
559 using PROTTEST3 (-JTT -LG -DCMut -Dayhoff –WAG -G -I -F -AIC –BIC;
560 https://github.com/ddarriba/prottest3; [82]) and iqTree's ModelFinder (-m MF -msub nuclear
561 -nt AUTO; [83]). Maximum-likelihood trees were generated using iqTree (opsins: -m LG+G -
562 bb 10000 -bnni -nt AUTO -alrt 10000 –abayes; CRY/PLs: -m LG+R6 -bb 10000 -bnni -nt
563 AUTO -alrt 10000 –abayes; [84]). Bayesian inference trees were calculated using MrBayes
564 (lset rates=gamma ngammacat=5; prset brlenspr=unconstrained:gammadir(1.0,0.1,1.0,1.0)
565 aamodelpr=fixed(lg);mcmc ngen=1100000 samplefreq=200 printfreq=1000 nchains=4
566 temp=0.2 savebrlens=yes; starttree=random;set seed=518; sumt burnin=500; sump
567 burnin=500; [85]). For opsin and CRY/PL phylogenies support values of resulting ML and
568 Baysian analyses were combined using Treegraph2.14.0-771 [86]. Resulting trees were
569 finalized using FigTree 1.4.4 (http://tree.bio.ed.ac.uk/software/figtree/) and Adobe Illustrator
570 CC 2018. All alignments, tree files and accession numbers are provided in nexus format
571 (Supplementary File 4-6).
572
573 *Domain structure analysis, sequence logos and duplicate domain confirmation*
574 The domain structures of the different CRYs and opsins were predicted using InterProScan
575 v5.44 in Geneious R10 (Biomatters). Sequence logos were generated using Weblogo [87].
576 Sequencing a region spanning exon 7 and 8, which encode the C-terminal end of the FAD-
577 binding domain of the AnthoCRY.1 PHR region 1 and the start of the N-terminal sequence of
578 the AnthoCRY.1 PHR region 2 confirmed the presence of the PHR region tandem
579 duplication. Here, RNA (as cDNA) and gDNA were PCR amplified using exon-specific
580 primers (Supplementary Table 1), cloned into pJET2.1 and then Sanger sequenced.
581 Alignment of sequenced fragments confirmed that the genomic sequence contains an intron
582 and that the genomic and transcript sequences of AnthoCRY.1 span two individual PHR
583 regions and that both are expressed.
584

16

585 *Conserved intron structure analysis*

586 Reference sequences were chosen at random to represent the canonical exon-intron structure

587 of the respective Opsin/CRY/PL types. Reference and *Aiptasia* opsin gene models were

588 generated using WebScipio [88] and conserved introns were identified using GenePainter 2.0

589 [89].

590

591 *Expression quantification of PLs, CRYs and opsins*

592 We analysed expression of the CRY, PL and opsin genes using the same published short read

593 RNA-seq libraries that we used for gene model verification comprising data for adult and

594 larval life stages from aposymbiotic and symbiotic states including 2-4 biological replicates

595 per sample treatment [90]. The ultra-fast, bias-aware short read mapper Salmon [91] and in-

596 house R scripts were used to generate a TMM normalised expression quantitation matrix

597 across all conditions and samples. Average expression data for adult and larval *Aiptaisa* was

598 used irrespective of their symbiotic state to analyse the differential developmental expression

599 of CRYs and opsins. To compare the effect of symbiosis, the average expression in symbiotic

600 and aposymbiotic adults was compared. Graphs were drawn and significance levels were

601 determined using a multiple t-test in Prism 8.1.1 (GraphPad).

602

603 *D-box and E-box searches*

604 Potential PAR/bZIP binding sites in the genomic region 1kb upstream of the CRY/PL TSS

605 were identified using MATCH 1.0 Public (http://gene-regulation.com/pub/programs.html)

606 (Binding sites for Hlf (TransFac ID: T01071) and VBP (TransFac ID: T00881) were

607 considered D-Boxes). The identified potential sites were aligned to the canonical D-Box

608 elements identified in zebrafish using ClustalW (GONNET, goc: 3, gec: 1.8). Statistically

609 overrepresented E-box motifs were identified in the same genomic regions using Clover [92]

610 and a library of 9 TF binding motifs including several know (MITF and USF TF binding

611 motifs) and one manually generated E-box motif. An approx. 6Mbp *Aiptasia* genomic

612 scaffold (Genbank Accession NW_018384103.1) was used as a background sequence.

613

614 **Gene expression**

615 *RNA extraction and qPCR*

616 For circadian rhythmicity qPCR analysis, polyps were macerated in Trizol at a concentration

617 of 500mg per ml, snap frozen in liquid nitrogen and stored at -80 °C. Total RNA was

618 extracted as described, but replacing phenol-chloroform with Trizol [37]. For determination

619 of opsin expression levels in mesentery and tentacle tissues, a number of adult male *Aiptasia*

620 were anesthetized in 7% $MgCl_2$ (w/v) in ASW (1:1) for 1 hour and then transferred into

621 Methacarn fixative (6:3:1 methanol:chloroform:acetic acid). Following two Methacarn

17

622 changes in the first hour the samples were then incubated for 48 hours at RT. Individual
623 polyps were then transferred into PBS and dissected to separate tentacle and mesentery
624 tissues. Total RNA was extracted from dissected tissue samples as described in Hambleton et
625 al. (2020) replacing phenol-chloroform with Trizol. In all cases cDNA was synthesised with 1
626 µg of total RNA per sample using a ReadyScript cDNA Synthesis Mix (Sigma-Aldrich).
627 Primers for qPCR were determined using NCBI Primer BLAST (standard settings optimised
628 for 100 bp exon-spanning amplicons) or designed manually using the same exon spanning
629 rules when NCBI gene models were not available (For qPCR primers see: Supplementary
630 Table 1). All qPCRs were run on a BioSystems StepOne Real-Time PCR System
631 (ThermoFisher) using a Luna Universal qPCR Master Mix (NEB) at the fast setting following
632 the manufacturer's instructions to determine dCT levels in triplicate. Genes encoding 40S
633 Ribosomal Proteins S7 and L11 (RPS7 and RPL11) and actin were chosen as
634 comparison/baseline genes. Primers were validated in triplicate by amplicon sequencing of
635 qPCR products. Melt curves were generated after each run confirming only a single product
636 per reaction. Amplification efficiencies of each primer pair were determined through dilution
637 series. Results were analysed according to a standard protocol
638 (https://matzlab.weebly.com/data--code.html) using in-house KNIME (www.knime.com)
639 workflows comprising an R integration of the Bayesian analysis pipeline MCMC.qPCR [93].
640

## Acknowledgments

## References:

1. Zapata F, Goetz FE, Smith SA, Howison M, Siebert S, Church SH, Sanders SM, Ames CL, McFadden CS, France SC, Daly M, Collins AG, Haddock SHD, Dunn CW, Cartwright P: **Phylogenomic Analyses Support Traditional Relationships within Cnidaria.** *PLoS ONE* 2015, **10**:e0139068.

2. Janouskovec J, Gavelis GS, Burki F, Dinh D, BACHVAROFF TR, Gornik SG, Bright KJ, Imanian B, Strom SL, Delwiche CF, Waller RF, Fensome RA, Leander BS, Rohwer FL, Saldarriaga JF: **Major transitions in dinoflagellate evolution unveiled by phylotranscriptomics**. *Proceedings of the National Academy of Sciences* 2017, **114**:E171–E180.

3. LaJeunesse TC, Parkinson JE, Gabrielson PW, Jeong HJ, Reimer JD, Voolstra CR, Santos SR: **Systematic Revision of Symbiodiniaceae Highlights the Antiquity and Diversity of Coral Endosymbionts.** *Curr Biol* 2018, **28**:2570–2580.e6.

661    4. Fisher R, O'Leary RA, Low-Choy S, Mengersen K, Knowlton N, Brainard RE, Caley MJ:
662    **Species Richness on Coral Reefs and the Pursuit of Convergent Global Estimates**.
663    *Current Biology* 2015, **25**:500–505.

664    5. Kaniewska P, Alon S, Karako-Lampert S, Hoegh-Guldberg O, Levy O: **Signaling cascades**
665    **and the importance of moonlight in coral broadcast mass spawning**. *doiorg* 2015.

666    6. Sweeney AM, Boch CA, Johnsen S, Morse DE: **Twilight spectral dynamics and the**
667    **coral reef invertebrate spawning response**. *J Exp Biol* 2011, **214**:770–777.

668    7. Kanaya HJ, Kobayakawa Y, Itoh TQ: **Hydra vulgaris exhibits day-night variation in**
669    **behavior and gene expression levels**. 2019:1–12.

670    8. Foo SA, Liddell L, Grossman A, Caldeira K: **Photo-movement in the sea anemone**
671    **Aiptasia influenced by light quality and symbiotic association**. *Coral Reefs* 2019, **39**:47–
672    54.

673    9. Bielecki J, Zaharoff AK, Leung NY, Garm A, Oakley TH: **Ocular and Extraocular**
674    **Expression of Opsins in the Rhopalium of Tripedalia cystophora (Cnidaria: Cubozoa)**.
675    *PLoS ONE* 2014, **9**:e98870.

676    10. Oakley TH, Speiser DI: **How Complexity Originates: The Evolution of Animal Eyes**.
677    *Annu Rev Ecol Evol Syst* 2015, **46**:237–260.

678    11. Suga H, Schmid V, Gehring WJ: **Evolution and functional diversity of jellyfish opsins.**
679    *Current Biology* 2008, **18**:51–55.

680    12. Picciani N, Kerlin JR, Sierra N, Swafford AJM, Ramirez MD, Roberts NG, Cannon JT,
681    Daly M, Oakley TH: **Prolific Origination of Eyes in Cnidaria with Co-option of Non-**
682    **visual Opsins**. *Current Biology* 2018, **28**:2413–2419.e4.

683    13. Levy O, Appelbaum L, Leggat W, Gothlif Y, Hayward DC, Miller DJ, Hoegh-Guldberg
684    O: **Light-responsive cryptochromes from a simple multicellular animal, the coral**
685    **Acropora millepora.** *Science* 2007, **318**:467–470.

686    14. Levy O, Kaniewska P, Alon S, Eisenberg E, Karako-Lampert S, Bay LK, Reef R,
687    Rodriguez-Lanetty M, Miller DJ, Hoegh-Guldberg O: **Complex Diel Cycles of Gene**
688    **Expression in Coral-Algal Symbiosis**. *Science* 2011, **331**:175–175.

689    15. Artigas GQ, Lapébie P, Leclère L, Takeda N, Deguchi R, Jékely G, Momose T, Houliston
690    E: **A gonad-expressed opsin mediates light-induced spawning in the jellyfish Clytia**.
691    *elifesciencesorg* 2018.

692    16. Macias-Muñoz A, Murad R, Mortazavi A: **Molecular evolution and expression of opsin**
693    **genes in Hydra vulgaris.** *BMC Genomics* 2019, **20**:1–19.

694    17. Terakita A: **The opsins.** *Genome Biol* 2005, **6**:213.

695    18. Plachetzki DC, Fong CR, Oakley TH: **The evolution of phototransduction from an**
696    **ancestral cyclic nucleotide gated pathway**. *Proceedings of the Royal Society B: Biological*
697    *Sciences* 2010, **277**:1963–1969.

698    19. Feuda R, Hamilton SC, McInerney JO, Pisani D: **Metazoan opsin evolution reveals a**
699    **simple route to animal vision**. *Proceedings of the National Academy of Sciences* 2012,
700    **109**:18868–18872.

20. Yokoyama H, Mizutani R: **Structural Biology of DNA (6-4) Photoproducts Formed by Ultraviolet Radiation and Interactions with Their Binding Proteins**. *IJMS* 2014, **15**:20321–20338.

21. Benjdia A: **DNA photolyases and SP lyase: structure and mechanism of light-dependent and independent DNA lyases.** *Curr Opin Struct Biol* 2012, **22**:711–720.

22. Cashmore AR: **Cryptochromes: Blue Light Receptors for Plants and Animals**. *Science* 1999, **284**:760–765.

23. Chaves I, Pokorny R, Byrdin M, Hoang N, Ritz T, Brettel K, Essen L-O, van der Horst GTJ, Batschauer A, Ahmad M: **The Cryptochromes: Blue Light Photoreceptors in Plants and Animals**. *Annu Rev Plant Biol* 2011, **62**:335–364.

24. Malhotra K, Kim ST, Batschauer A, Dawut L, Sancar A: **Putative blue-light photoreceptors from Arabidopsis thaliana and Sinapis alba with a high degree of sequence homology to DNA photolyase contain the two photolyase cofactors but lack DNA repair activity.** *Biochemistry* 1995, **34**:6892–6899.

25. Lucas-Lledo JI, Lynch M: **Evolution of Mutation Rates: Phylogenomic Analysis of the Photolyase/Cryptochrome Family**. *Molecular Biology and Evolution* 2009, **26**:1143–1153.

26. Sancar A: **Structure and function of DNA photolyase and cryptochrome blue-light photoreceptors.** *Chem Rev* 2003, **103**:2203–2237.

27. Stanewsky R, Kaneko M, Emery P, Beretta B, Wager-Smith K, Kay SA, Rosbash M, Hall JC: **The cryb mutation identifies cryptochrome as a circadian photoreceptor in Drosophila.** *Cell* 1998, **95**:681–692.

28. Thompson CL, Sancar A: **Photolyase/cryptochrome blue-light photoreceptors use photon energy to repair DNA and reset the circadian clock.** *Oncogene* 2002, **21**:9043–9056.

29. Emery P, So WV, Kaneko M, Hall JC, Rosbash M: **CRY, a Drosophila clock and light-regulated cryptochrome, is a major contributor to circadian rhythm resetting and photosensitivity.** *Cell* 1998, **95**:669–679.

30. Kume K, Zylka MJ, Sriram S, Shearman LP, Weaver DR, Jin X, Maywood ES, Hastings MH, Reppert SM: **mCRY1 and mCRY2 are essential components of the negative limb of the circadian clock feedback loop.** *Cell* 1999, **98**:193–205.

31. Shearman LP, Sriram S, Weaver DR, Maywood ES, Chaves I, Zheng B, Kume K, Lee CC, van der Horst GT, Hastings MH, Reppert SM: **Interacting molecular loops in the mammalian circadian clock.** *Science* 2000, **288**:1013–1019.

32. Gindt YM, Messyasz A, Jumbo PI: **Binding of Substrate Locks the Electrochemistry of CRY-DASH into DNA Repair**. *Biochemistry* 2015, **54**:2802–2805.

33. Weis VM, Davy SK, Hoegh-Guldberg O, Rodriguez-Lanetty M, Pringle JR: **Cell biology in model systems as the key to understanding corals.** *Trends in Ecology & Evolution* 2008, **23**:369–376.

34. Wolfowicz I, Baumgarten S, Voss PA, Hambleton EA, Voolstra CR, Hatta M, Guse A: **Aiptasia sp. larvae as a model to reveal mechanisms of symbiont selection in cnidarians.** *Sci Rep* 2016, **6**:32366.

742   35. Neubauer E-F, Poole AZ, Neubauer P, Detournay O, Tan K, Davy SK, Weis VM: **A**
743   **diverse host thrombospondin-type-1 repeat protein repertoire promotes symbiont**
744   **colonization during establishment of cnidarian-dinoflagellate symbiosis.** *Elife* 2017, **6**:1–
745   26.

746   36. Matthews JL, Crowder CM, Oakley CA, Lutz A, Roessner U, Meyer E, Grossman AR,
747   Weis VM, Davy SK: **Optimal nutrient exchange and immune responses operate in**
748   **partner specificity in the cnidarian-dinoflagellate symbiosis**. *Proceedings of the National*
749   *Academy of Sciences* 2017, **114**:13194–13199.

750   37. Hambleton EA, Jones VAS, Maegele I, Kvaskoff D, Sachsenheimer T, Guse A: **Sterol**
751   **transfer by atypical cholesterol-binding NPC2 proteins in coral-algal symbiosis**.
752   *elifesciencesorg* 2019.

753   38. Bucher M, Wolfowicz I, Voss PA, Hambleton EA, Guse A: **Development and Symbiosis**
754   **Establishment in the Cnidarian Endosymbiosis Model Aiptasia sp.** *Sci Rep* 2016,
755   **6**:19867.

756   39. Tolleter D, Seneca FO, DeNofrio JC, Krediet CJ, Palumbi SR, Pringle JR, Grossman AR:
757   **Coral bleaching independent of photosynthetic activity.** *Curr Biol* 2013, **23**:1782–1786.

758   40. Grawunder D, Hambleton EA, Bucher M, Wolfowicz I, Bechtoldt N, Guse A: **Induction**
759   **of Gametogenesis in the Cnidarian Endosymbiosis Model Aiptasia sp.** *Sci Rep* 2015,
760   **5**:15677.

761   41. Arendt D: **Ciliary Photoreceptors with a Vertebrate-Type Opsin in an Invertebrate**
762   **Brain**. *Science* 2004, **306**:869–871.

763   42. Vöcking O, Kourtesis I, Tumu SC, Hausen H: **Co-expression of xenopsin and**
764   **rhabdomeric opsin in photoreceptors bearing microvilli and cilia**. *elifesciencesorg* 2017.

765   43. Plachetzki DC, Fong CR, Oakley TH: **Cnidocyte discharge is regulated by light and**
766   **opsin-mediated phototransduction.** *BMC Biol* 2012, **10**:17.

767   44. Musilova Z, Cortesi F, Matschiner M, Davies WIL, Patel JS, Stieb SM, de Busserolles F,
768   Malmstrøm M, Tørresen OK, Brown CJ, Mountford JK, Hanel R, Stenkamp DL, Jakobsen
769   KS, Carleton KL, Jentoft S, Marshall J, Salzburger W: **Vision using multiple distinct rod**
770   **opsins in deep-sea fishes**. *Science* 2019, **364**:588–592.

771   45. Hope AJ, Partridge JC, Dulai KS, Hunt DM: **Mechanisms of wavelength tuning in the**
772   **rod opsins of deep-sea fishes**. *Proceedings of the Royal Society B: Biological Sciences* 1997,
773   **264**:155–163.

774   46. Hunt DM, Dulai KS, Partridge JC, Cottrill P, Bowmaker JK: **The molecular basis for**
775   **spectral tuning of rod visual pigments in deep-sea fish**. *J Exp Biol* 2001, **204**:3333–3344.

776   47. Imai H, Kojima D, Oura T, Tachibanaki S, Terakita A, Shichida Y: **Determinants of**
777   **visual pigment absorbance: identification of the retinylidene Schiff's base counterion in**
778   **bovine rhodopsin**. *Proceedings of the National Academy of Sciences* 1997, **94**:2322–2326.

779   48. Terakita A, Nagata T: **Functional Properties of Opsins and their Contribution to**
780   **Light-Sensing Physiology**. *Zoological Science* 2014, **31**:653–659.

781   49. Terakita A, Yamashita T, Shichida Y: **Highly conserved glutamic acid in the**
782   **extracellular IV-V loop in rhodopsins acts as the counterion in retinochrome, a member**

783     **of the rhodopsin family.** *Proc Natl Acad Sci USA* 2000, **97**:14263–14267.

784     50. Sakmar TP, Franke RR, Khorana HG: **Glutamic acid-113 serves as the retinylidene**
785     **Schiff base counterion in bovine rhodopsin.** *Proc Natl Acad Sci USA* 1989, **86**:8309–8313.

786     51. Zhukovsky E, Oprian D: **Effect of carboxylic acid side chains on the absorption**
787     **maximum of visual pigments**. *Science* 1989, **246**:928–930.

788     52. Tsutsui K, Shichida Y: **Multiple functions of Schiff base counterion in rhodopsins.**
789     *Photochem Photobiol Sci* 2010, **9**:1426–1434.

790     53. Gerrard E, Mutt E, Nagata T, Koyanagi M, Flock T, Lesca E, Schertler GFX, Terakita A,
791     Deupi X, Lucas RJ: **Convergent evolution of tertiary structure in rhodopsin visual**
792     **proteins from vertebrates and box jellyfish.** *Proceedings of the National Academy of*
793     *Sciences* 2018, **115**:6201–6206.

794     54. Baumgarten S, Simakov O, Esherick LY, Liew YJ, Lehnert EM, Michell CT, Li Y,
795     Hambleton EA, Guse A, Oates ME, Gough J, Weis VM, Aranda M, Pringle JR, Voolstra CR:
796     **The genome of Aiptasia, a sea anemone model for coral symbiosis**. *Proceedings of the*
797     *National Academy of Sciences* 2015, **112**:11893–11898.

798     55. Gorbunov MY, Falkowski PG: **Photoreceptors in the cnidarian hosts allow symbiotic**
799     **corals to sense blue moonlight**. *Limnol Oceanogr* 2002, **47**:309–315.

800     56. Michael AK, Fribourgh JL, Van Gelder RN, Partch CL: **Animal Cryptochromes:**
801     **Divergent Roles in Light Perception, Circadian Timekeeping and Beyond**. *Photochem*
802     *Photobiol* 2017, **93**:128–140.

803     57. Lin C, Todo T: **The cryptochromes.** *Genome Biol* 2005, **6**:220.

804     58. Rivera AS, Ozturk N, Fahey B, Plachetzki DC, Degnan BM, Sancar A, Oakley TH: **Blue-**
805     **light-receptive cryptochrome is expressed in a sponge eye lacking neurons and opsin.** *J*
806     *Exp Biol* 2012, **215**:1278–1286.

807     59. Reitzel AM, Behrendt L, Tarrant AM: **Light Entrained Rhythmic Gene Expression in**
808     **the Sea Anemone Nematostella vectensis: The Evolution of the Animal Circadian Clock**.
809     *PLoS ONE* 2010, **5**:e12805.

810     60. Sorek M, Schnytzer Y, Ben-Asher HW, Caspi VC, Chen C-S, Miller DJ, Levy O: **Setting**
811     **the pace: host rhythmic behaviourand gene expression patterns in thefacultatively**
812     **symbiotic cnidarian Aiptasiaare determined largely by Symbiodinium**. 2018:1–12.

813     61. Zhao H, Di Mauro G, Lungu-Mitea S, Negrini P, Guarino AM, Frigato E, Braunbeck T,
814     Ma H, Lamparter T, Vallone D, Bertolucci C, Foulkes NS: **Modulation of DNA Repair**
815     **Systems in Blind Cavefish during Evolution in Constant Darkness.** *Curr Biol* 2018,
816     **28**:3229–3243.e4.

817     62. Mracek P, Santoriello C, Idda ML, Pagano C, Ben-Moshe Z, Gothilf Y, Vallone D,
818     Foulkes NS: **Regulation of per and cry Genes Reveals a Central Role for the D-Box**
819     **Enhancer in Light-Dependent Gene Expression**. *PLoS ONE* 2012, **7**:e51278.

820     63. Vatine G, Vallone D, Appelbaum L, Mracek P, Ben-Moshe Z, Lahiri K, Gothilf Y,
821     Foulkes NS: **Light Directs Zebrafish period2 Expression via Conserved D and E Boxes**.
822     *Plos Biol* 2009, **7**:e1000223.

823   64. Pagano C, Siauciunaite R, Idda ML, Ruggiero G, Ceinos RM, Pagano M, Frigato E,
824   Bertolucci C, Foulkes NS, Vallone D: **Evolution shapes the responsiveness of the D-box**
825   **enhancer element to light and reactive oxygen species in vertebrates.** *Sci Rep* 2018,
826   **8**:13180.

827   65. Gachon F, Olela FF, Schaad O, Descombes P, Schibler U: **The circadian PAR-domain**
828   **basic leucine zipper transcription factors DBP, TEF, and HLF modulate basal and**
829   **inducible xenobiotic detoxification.** *Cell Metab* 2006, **4**:25–36.

830   66. Mitsui S: **Antagonistic role of E4BP4 and PAR proteins in the circadian oscillatory**
831   **mechanism**. *Genes & Development* 2001, **15**:995–1006.

832   67. Ramirez MD, Pairett AN, Pankey MS, Serb JM, Speiser DI, Swafford AJ, Oakley TH:
833   **The last common ancestor of most bilaterian animals possessed at least 9 opsins**. *Genome*
834   *Biol Evol* 2016:evw248.

835   68. Cunningham A, Ramage L, McKee D: **Relationships between inherent optical**
836   **properties and the depth of penetration of solar radiation in optically complex coastal**
837   **waters**. *J Geophys Res Oceans* 2013, **118**:2310–2317.

838   69. Renema W: **Accepted Manuscript**. *Earth-Science Reviews* 2017:1–104.

839   70. Sekharan S, Altun A, Morokuma K: **Photochemistry of Visual Pigment in a G q**
840   **Protein-Coupled Receptor (GPCR)-Insights from Structural and Spectral Tuning**
841   **Studies on Squid Rhodopsin**. *Chem Eur J* 2010, **16**:1744–1749.

842   71. Shlesinger T, Loya Y: **Breakdown in spawning synchrony: A silent threat to coral**
843   **persistence**. *Science* 2019, **365**:1002–1007.

844   72. Jones VAS, Bucher M, Hambleton EA, Guse A: **Microinjection to deliver protein,**
845   **mRNA, and DNA into zygotes of the cnidarian endosymbiosis model Aiptasia sp.** *Sci Rep*
846   2018, **8**:679–11.

847   73. Reitzel AM, Tarrant AM, Levy O: **Circadian Clocks in the Cnidaria: Environmental**
848   **Entrainment, Molecular Regulation, and Organismal Outputs**. *Integr Comp Biol* 2013,
849   **53**:118–130.

850   74. Bozek K, Relógio A, Kielbasa SM, Heine M, Dame C, Kramer A, Herzel H: **Regulation**
851   **of Clock-Controlled Genes in Mammals**. *PLoS ONE* 2009, **4**:e4882.

852   75. Chapman JA, Kirkness EF, Simakov O, Hampson SE, Mitros T, Weinmaier T, Rattei T,
853   Balasubramanian PG, Borman J, Busam D, Disbennett K, Pfannkoch C, Sumin N, Sutton GG,
854   Viswanathan LD, Walenz B, Goodstein DM, Hellsten U, Kawashima T, Prochnik SE, Putnam
855   NH, Shu S, Blumberg B, Dana CE, Gee L, Kibler DF, Law L, Lindgens D, Martinez DE,
856   Peng J, et al.: **The dynamic genome of Hydra.** *Nature* 2010, **464**:592–596.

857   76. Oren M, Tarrant AM, Alon S, Simon-Blecher N, Elbaz I, Appelbaum L, Levy O:
858   **Profiling molecular and behavioral circadian rhythms in the non-symbiotic sea anemone**
859   **Nematostella vectensis.** *Sci Rep* 2015, **5**:11418.

860   77. Brudler R, Hitomi K, Daiyasu H, Toh H, Kucho K-I, Ishiura M, Kanehisa M, Roberts VA,
861   Todo T, Tainer JA, Getzoff ED: **Identification of a New Cryptochrome Class**. *Molecular*
862   *Cell* 2003, **11**:59–67.

863   78. Kim D, Langmead B, Salzberg SL: **HISAT: a fast spliced aligner with low memory**

864     **requirements**. *Nat Methods* 2015, **12**:357–360.

865     79. Kayal E, Bentlage B, Pankey MS, Ohdera AH, Medina M, Plachetzki DC, Collins AG,
866     Ryan JF: **Phylogenomics provides a robust topology of the major cnidarian lineages and**
867     **insights on the origins of key organismal traits**. 2018:1–18.

868     80. Capella-Gutierrez S, Silla-Martinez JM, Gabaldon T: **trimAl: a tool for automated**
869     **alignment trimming in large-scale phylogenetic analyses**. *Bioinformatics* 2009, **25**:1972–
870     1973.

871     81. Smith SA, Dunn CW: **Phyutility: a phyloinformatics tool for trees, alignments and**
872     **molecular data**. *Bioinformatics* 2008, **24**:715–716.

873     82. Darriba D, Taboada GL, Doallo R, Posada D: **ProtTest 3: fast selection of best-fit**
874     **models of protein evolution**. *Bioinformatics* 2011, **27**:1164–1165.

875     83. Kalyaanamoorthy S, Minh BQ, Wong TKF, Haeseler von A, Jermiin LS: **ModelFinder:**
876     **fast model selection for accurate phylogenetic estimates**. *Nat Methods* 2017, **14**:587–589.

877     84. Nguyen L-T, Schmidt HA, Haeseler von A, Minh BQ: **IQ-TREE: a fast and effective**
878     **stochastic algorithm for estimating maximum-likelihood phylogenies.** *Molecular Biology*
879     *and Evolution* 2015, **32**:268–274.

880     85. Ronquist F, Teslenko M, van der Mark P, Ayres DL, Darling A, Höhna S, Larget B, Liu
881     L, Suchard MA, Huelsenbeck JP: **MrBayes 3.2: efficient Bayesian phylogenetic inference**
882     **and model choice across a large model space.** *Systematic Biology* 2012, **61**:539–542.

883     86. Stöver BC, Müller KF: **TreeGraph 2: Combining and visualizing evidence from**
884     **different phylogenetic analyses**. *BMC Bioinformatics* 2010, **11**:275.

885     87. Crooks GE, Hon G, Chandonia J-M, Brenner SE: **WebLogo: a sequence logo generator.**
886     *Genome Research* 2004, **14**:1188–1190.

887     88. Odronitz F, Pillmann H, Keller O, Waack S, Kollmar M: **WebScipio: An online tool for**
888     **the determination of gene structures using protein sequences**. *BMC Genomics* 2008,
889     **9**:422.

890     89. Mühlhausen S, Hellkamp M, Kollmar M: **GenePainter v. 2.0 resolves the taxonomic**
891     **distribution of intron positions**. *Bioinformatics* 2014, **31**:1302–1304.

892     90. Lehnert EM, Mouchka ME, Burriesci MS, Gallo ND, Schwarz JA, Pringle JR: **Extensive**
893     **differences in gene expression between symbiotic and aposymbiotic cnidarians.** *G3*
894     *(Bethesda)* 2014, **4**:277–295.

895     91. Patro R, Duggal G, Love MI, Irizarry RA, Kingsford C: **Salmon provides fast and bias-**
896     **aware quantification of transcript expression**. *Nat Methods* 2017, **14**:417–419.

897     92. Frith MC: **Detection of functional DNA motifs via statistical over-representation**.
898     *Nucleic Acids Research* 2004, **32**:1372–1381.

899     93. Matz MV, Wright RM, Scott JG: **No Control Genes Required: Bayesian Analysis of**
900     **qRT-PCR Data**. *PLoS ONE* 2013, **8**:e71448.

901     94. Davies WL, Hankins MW, Foster RG: **Vertebrate ancient opsin and melanopsin:**
902     **divergent irradiance detectors**. *Photochem Photobiol Sci* 2010, **9**:1444.

903 **Figure legends**

904 **Figure 1: The cnidarian lifestyle is dominated by sun- and moonlight**

905 (A) Cladogram revealing phylogenetic relations within the phylum cnidaria showing the two

906 main classes Anthozoa and Medusozoa and their major subclasses. (B) Schematic overview

907 of how environmental light impacts (symbiotic) cnidarians throughout life from embryo to

908 adult. Light by the moon induces spawning and synchronizes gamete release. Larvae then use

909 environmental light for orientation and during settlement. Adults change behaviour in

910 response to light to modulate photosynthesis rates of symbionts, to seek shelter from UV

911 radiation or for predator avoidance.

912

913 **Figure 2: Anthozoa retained the most ancient animal opsin classes and evolved a novel**

914 **sub-group (actinarian ASO-IIs)**

915 (A) Consensus tree topology generated with IQTree reveals that cnidarians have at least 3

916 opsin paralogs. Anthozoans possess ASO-Is and ASO-IIs, which are monophyletic. ASO-I

917 appears ancestral to all other animal opsins. All cnidarians (Anthozoa and Medusozoa)

918 possess cnidopsins. Cnidopsins are monophyletic also and sister to the animal xenopsins.

919 ASO-IIs contain two distinct sub-clusters. The first cluster comprises solely *Actiniaria* (sea

920 anemone) sequences and we named this grouping 'Actiniarian ASO-IIs' while the second

921 cluster contains genes from all Anthozoa families including corals. Intron phase analysis

922 suggests that ASO-IIs and Actiniarian ASO-IIs both are distinct from ctenopsin and c-opsin

923 gene structures despite their common ancestry lacking any conserved homologous intron

924 positions (Supplementary Figure 1A). Note: *C. hemispherica* opsin 9 and opsin 10 resolve at

925 the base of the ASO-IIs, however elsewhere they are included within the cnidopsins albeit

926 with long branches [15]. Support values are (SH-aLRT boostrap percentages/UFBoots

927 boostrap percentages/aBayes Bayesian posterior probabilities). Branch length is proportional

928 to substitutions per site. (B) Bayesian topology tree generated with MrBayes using an

929 expanded ASO-II dataset (Picciani et al. (2018)) confirms the ASO-II/actiniarian ASO-II sub-

930 clustering. Branch length is proportional to substitutions per site. (A) + (B) Full trees can be

931 accessed through Supplementary File 4. (C) Sequence logo showing that most actiniarian

932 ASO-IIs possess a typical primary counter ion (glutamic acid [E]) at position 181; all other

933 ASO-IIs lack this counter ion. The separation of the two ASO-groupings is also reflected in

934 their intron phasing: both ASO-II groupings possess distinct homologous introns

935 (Supplementary Figure 1B).

936

937

938 **Figure 3: Expression profiles of *Aiptasia* opsins varies between life-stages and symbiotic**
939 **state**

940 (A) Bar chart comparing the expression (TMM normalised reads) of *Aiptasia* opsins in adults
941 and larva. ASO-I.2, ASO-II.2, ASO-II.3, ASO-II.5 and ASO-II.12 are significantly
942 upregulated in larva. ASO-II.8, ASO-II.9 and ASO-II.11 are significantly upregulated in
943 adults. (B) Bar chart comparing the expression (TMM normalised reads) of *Aiptasia* opsins in
944 symbiotic and aposymbiotic adults. ASO-II.12, ASO-II.7 and ASO-II.11 are significantly
945 upregulated in symbiotic adults. (C) Tissue-specific qPCR after Methacarn fixation of adult
946 *Aiptasia* polyps reveals that ASO-II.3 is significantly upregulated in mesenteries, when
947 compared with tentacle tissue. Data for all other opsins are shown in Supplementary Figure 3.
948 For all charts significant differences are: * P ≤ 0.05, ** P ≤ 0.01, *** P ≤ 0.001; and error
949 bars are: SEM.

950

951

952 **Figure 4: PL and CRY phylogeny reveals a novel, Anthozoan-specific CRY class**
953 (A) Consensus tree topology generated with IQTree reveals that PLs (CPD-II, PLs and (6-4)
954 PLs) and CRY-DASHs are common amongst all Cnidaria. Other CRYs including CRY-II
955 occur only in Anthozoa but are entirely absent from Medusozoa. The present phylogeny is
956 supported by highly conserved and specific exon-intron patterns (Supplementary Figure X)
957 suggesting that CRY-IIs and (6-4) PLs share a common origin. A well supported but
958 previously unidentified, anthozoan-specific CRY family resolves at the base of animal CRY-
959 IIs and (6-4) PLs which we name Anthozoan-specific CRYs (AnthoCRYs). Support values
960 are (SH-aLRT boostrap percentages/UFBoots boostrap percentages/aBayes Bayesian
961 posterior probabilities). A full tree can be accessed through Supplementary File 5. (B)
962 Cryptochromes (except CRY-DASH) are absent in Medusozoa, while the Anthozoa possess a
963 novel class of cryptochromes (AnthoCRYs), which contain unique tandem duplications
964 including up to 6 copies of the PHR region comprising the N-terminal DNA-binding
965 photolyase domain (also called alpha/beta domain, red) and the chromophore-binding FAD
966 domain (grey). (C) A comparison between cDNA- and genomic DNA-derived exon spanning
967 amplicon sequencing confirms PHR region duplication in *Aiptasia* AnthoCRY.1
968 (XP_020902079).

969

970

971 **Figure 5: Light-induced expression profiles of *Aiptasia* CRYs and PLs**
972 (A) – (F) qPCR analysis of CRY and PL gene expression in response to light exposure in
973 adult *Aiptasia*. Animals were adapted for 4 days to constant darkness and then exposed to
974 light for a period of 8 hours; sampling every 2 hours. Control animals were kept in constant

975    darkness. *Aiptasia* CPD-II, *Aiptasia* DASH-CRY and *Aiptasia* (6-4) PL are unresponsive to

976    light treatment. AnthoCRY.1, AnthoCRY.1 and CRY-II expression is rapidly induced by

977    light. (G) – (I) qPCR analysis of CRY-II, AnthoCRY.1 and AnthoCRY.2 expression in LD-

978    adapted *Aiptasia* polyps. Animals were exposed to light-dark (LD, 12 hours:12 hours) cycles

979    and then transferred to constant darkness (DD), sampling at 2, 8, 14 and 20 hours (LD) and

980    26, 32, 38 and 44 hours (DD). Under LD conditions, we observed rhythmic expression with

981    elevated expression, peaking at 8 hours after lights on, and then decreasing during the dark

982    period, with a trough at 8 hours after lights off. In contrast, immediately upon transfer to DD

983    conditions, rhythmic expression was absent. (A) - (I) ANOVA was performed to confirm

984    statistically significant differences at each time point; $P < 0.01$. (J) Schematic representation

985    of the D- and E-box distribution (green and red boxes respectively) in *Aiptasia* PL and CRY

986    promoter regions extending up to 1000 bp upstream from the ATG start codons.

987

988    **Supplementary Figure 1: Intron phase analysis of opsin genes and summary table**

989    **showing conserved structural and functional opsin motifs in *Aiptasia***

990    (A) Intron phase analysis of all *Aiptasia* opsins showing that the type-specific introns in

991    Actiniarian ASO-IIs and ASO-IIs are conserved not only by position but also by intron phase

992    (red boxes). (B) Summary table showing conserved structural and functional opsin motifs in

993    *Aiptasia* in comparison to bovine rhodopsin and *Xenopus* melanopsin. These include: (i) two

994    conserved cysteine (C) residues at positions 110 and 187, which are involved in disulphide-

995    bond formation; (ii) two conserved glutamate [E] at position 113 and 181, which act as

996    negative counterion to the proton of the Schiff base and may also affect spectral tuning; (iii) a

997    glutamate [E] at position 134 located within a conserved motif (134–136; ERY in rhodopsin)

998    that provides a negative charge to stabilise the inactive opsin molecule; (iv) a conserved

999    lysine [K] at position 296 that is covalently linked to the 11-cis retinal chromophore via a

1000    Schiff base; (v) a conserved NPxxYx motif (302–313), which in rhodopsin contains a NKQ

1001    motif (310–312) that assists in maintaining structural integrity upon photopigment activation.

1002    The approximate position of the transmembrane domains is also depicted; modified from

1003    [94].

1004

1005    **Supplementary Figure 2: Distance matrix**

1006    Distance matrix reflecting an alignment of 577 animal opsins. Note that opsins are clustered

1007    by amino acid similarity and are not sorted based on phylogenetic distance only but overall

1008    sequence similarity. Cnidarian opsin paralog clusters are highlighted and their names colour

1009    coded.

1010

1011 **Supplementary Figure 3: Extended expression profiles of *Aiptasia* opsins in mesentery**

1012 **and tentacle tissue**

1013 qPCR analysis of mesentery and tentacle tissue after Methacarn fixation of adult *Aiptasia*

1014 polyps. ASO-I.2, ASO-II.1, ASO-II.4, Cnidopsin.3 and ASO_II.7 are significantly

1015 upregulated in tentacle tissue. ASO-II.3 is significantly upregulated in mesenteries.

1016 Cnidopsin.4 expression was not detected; ** $P \leq 0.01$; error bars are: SEM.

1017

1018 **Supplementary Figure 4: Intron phase analysis of PL and CRY genes and expression**

1019 **profiles of *Aiptasia* PLs and CRYs in larva and adults** (A) Intron phase analysis of all

1020 *Aiptasia* PLs and CRYs showing that select introns in CPDs, CRY-DASHs, CRY-Is,

1021 AnthoCRYs, animal CRY-IIs including Anthozoan CRY-IIs, and (6-4) PLs are conserved not

1022 only by position but also by intron phase (red boxes). (B) Bar chart comparing the expression

1023 (TMM normalised reads) of *Aiptasia* PLs and CRYs in adults and larva. AnthoCRY.2 is

1024 significantly upregulated in adults; ** $P \leq 0.01$.

1025

1026 **Supplementary Figure 5: *Aiptasia* PAR-bZIP TF phylogeny**

1027 Maximum-likelihood tree generated with iqTree reveals that *Aiptasia* (*E. pallida* in the tree)

1028 possesses four PAR-bZIP TFs: three TFs basal to HLF-type PAR/bZIP TFs and one DBP TF.

1029 The alignments and tree file including accession numbers are provided in nexus format
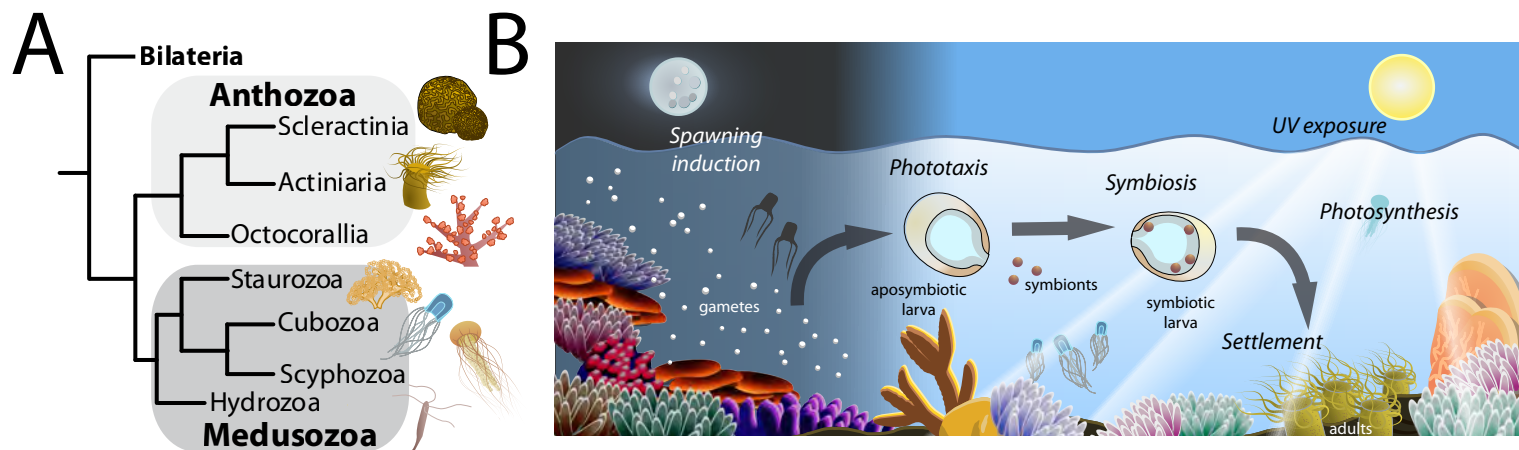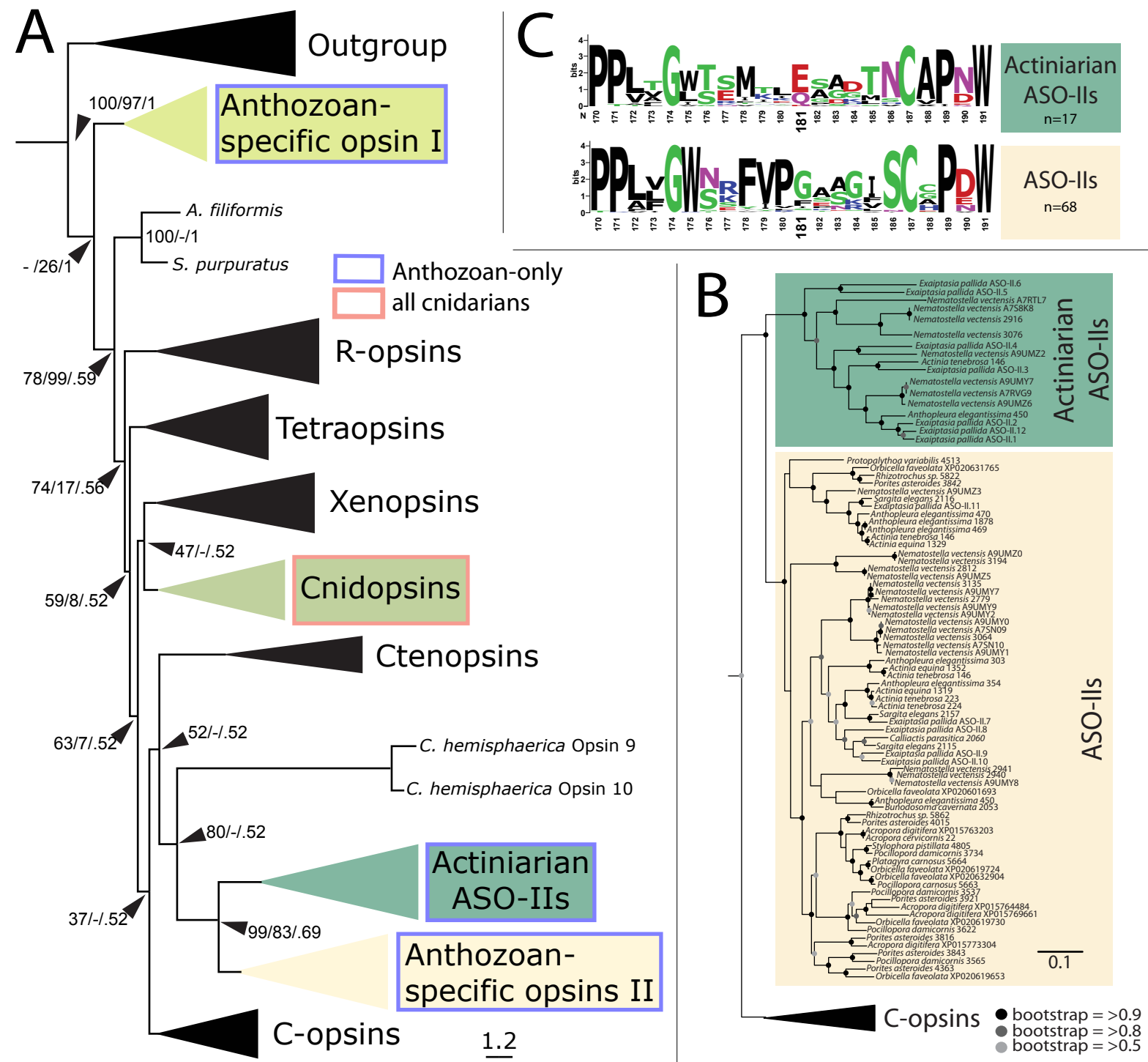
1030 (Supplementary File 6).

Figure 1

**A**
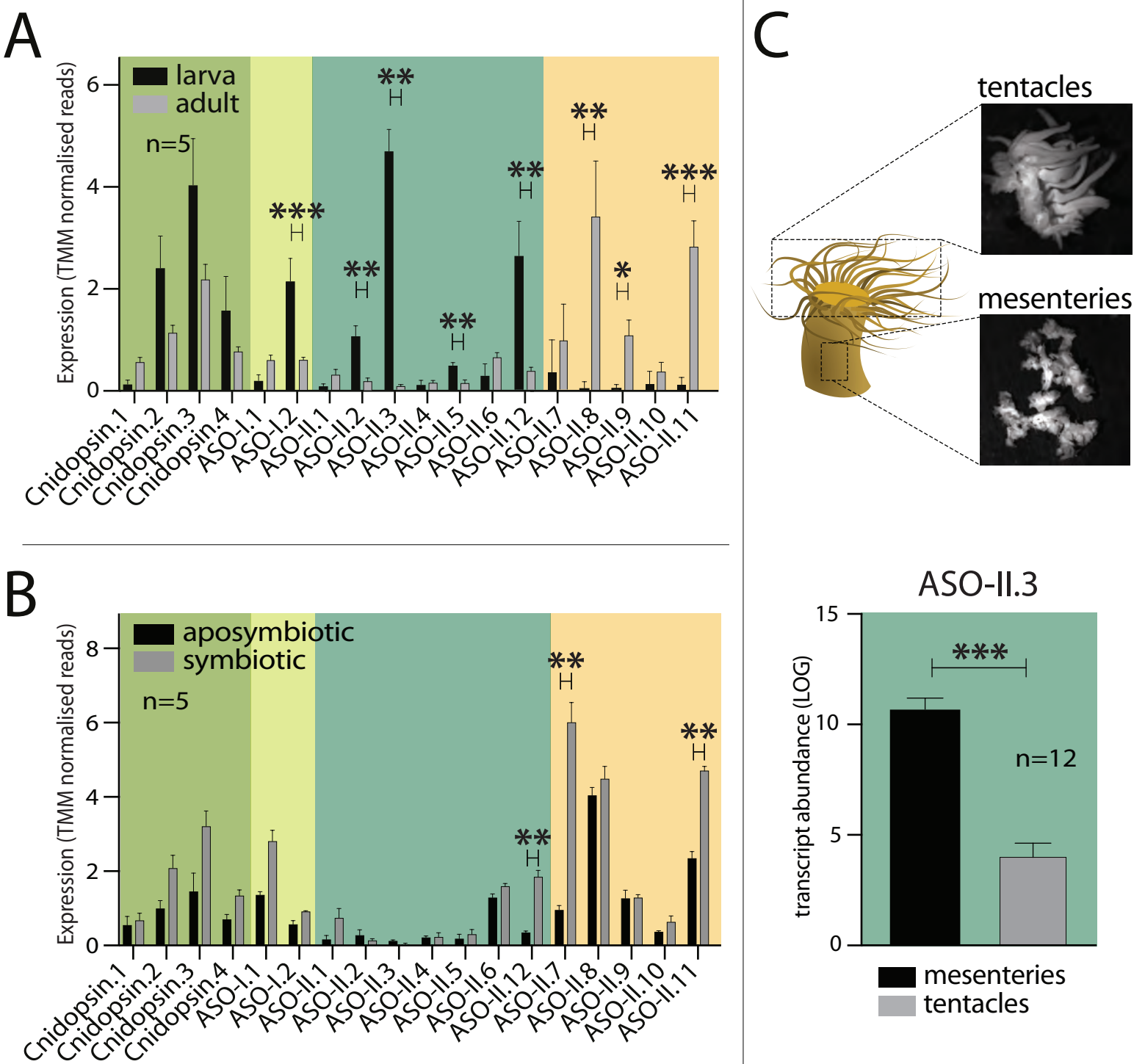
- Bilateria
- **Anthozoa**
  - Scleractinia
  - Actiniaria
  - Octocorallia
- Staurozoa
- Cubozoa
- Scyphozoa
- Hydrozoa
- **Medusozoa**

**B**

Figure 2

**Figure 3**

# Figure 4

Figure 5